ZDZISŁAW ZATORSKI [*]

EXPERIMENTAL VERIFICATION OF NUMERICAL SIMULATION OF PROJECTILE IMPACT ON BALLISTIC SHIELDS

In this work, the author presents experimental verification of numerical simulation of projectile impact on constructional shields. The experimental tests were performed at a unified test stand to investigate ballistic resistance of materials in field conditions. The stand was developed at the Polish Naval Academy in Gdynia, and then patented. The design of this test stand was based on construction of a ballistic pendulum, fitted to measure: impact force, turn angle of the ballistic pendulum χ, impact velocity and residual velocity of the projectile. All the measurement data were transmitted to a digital oscilloscope and a personal computer. The ballistic velocity of the shield of $V_{BL[R]}$ – defined according to Recht's and Ipson's method, was compared with $V_{BL[Z]}$ and $V_{BL[Z1]}$ – determined according to the author's method. Verification of numerically simulated ballistic velocity VRO versus the before-mentioned velocity was carried out at the 10GHMBA-E620T steel shields impacted by 12.7 mm type B-32 projectiles. The introduced method can be used for determining ballistic thickness h_{BL} and ballistic velocity V_{BL} for both homogeneous plates as well as multi-layered constructional shields.

Nomenclature

E_{BL} — ballistic energy absorbed by the shield and the projectile, $m_{BL}V_{BL}^2/2$, [kg m^2 s^{-2}],

E_p — kinetic energy of the projectile impact, $m_p V_p^2/2$, [kg m^2 s^{-2}],

h_{BL} — ballistic thickness, [m],

I — impulse of force transmitted to the dynamometer of the ballistic pendulum, [Ns],

J — polar moment of inertia, [kgm^2],

l — radius of rotation, [m],

---

[*] *Faculty of Mechanical and Electrical Engineering, Polish Naval Academy of Gdynia, J. Śmidowicza 69, 81-103 Gdynia, Poland; E-mail: z.zatorski@amw.gdynia.pl*

M_{ew}	–	equivalent mass of the pendulum, [kg],
m_{BL}	–	equivalent ballistic mass, [kg],
m_{ri}	–	residual mass of i-th projectile and shield fragment, [kg],
$m_{ri} \cdot V_{ri} \cdot \cos \phi_i$	–	residual momentum of the i-th fragment in the shot direction, [kgms^{-1}],
m_p	–	initial mass of the projectile, [kg],
m_{sp}, m_{st}	–	residual masses of the projectile and the shield which are remaining in the shield, [kg],
m_{rp}, m_{rt}	–	residual masses of the projectile and the shield which are running away from the shield, [kg],
V_{BL}	–	ballistic velocity of the shield, $V_r = 0$, [ms^{-1}],
$V_{BL[RI]}$	–	ballistic velocity of the shield according to Recht's and Ipson's method, [ms^{-1}],
$V_{BL[Z,Z1]}$	–	ballistic velocity of the shield according to author's method, [ms^{-1}],
V_p	–	impact velocity, [ms^{-1}],
V_r	–	residual velocity, [ms^{-1}],
V_w	–	velocity of the pendulum, [ms^{-1}],
ω_w	–	angular velocity of the ballistic pendulum, [s^{-1}],
χ	–	turn angle of the ballistic pendulum,
A, B	–	experimental constants.

1. Introduction

Kinetic energy of the projectile is transmitted to the shield, where it is transformed into plastic strain energy, thermal energy and the kinetic energy of particular components of the system. The behaviour of armour plates impacted by projectiles, for velocities including and exceeding ballistic limits, were preliminary investigated according to the following approaches: controlled experimentation, estimation of residual velocity and ballistic limit or ballistic velocity as a measurement of ballistic resistance of the material, with the aid of semi-empirical and limit-state solutions, and finite element-based contact-impact analysis.

2. Theoretical basis

The author postulates the following equations of the unified test stand behaviour with the fulfilment of conservation mass, momentum, moment of momentum and energy

$$m_p + m_t = m_r + m_s, \text{[kg]} \tag{1}$$

$$m_p \cdot V_p - m_s \cdot V_w - B \cdot m_r \cdot V_r = I, \text{[kgms}^{-1}] \tag{2}$$

$$J \cdot \omega_w = I \cdot l, \text{[kgm}^2 \text{s}^{-1}] \tag{3}$$

$$\frac{m_p \cdot V_P^2}{2} = \frac{m_{BL} \cdot V_{BL}^2}{2} + \frac{A \cdot m_r \cdot V_r^2}{2} + \frac{I^2}{2M_{ew}}, \text{[kgm}^2 \text{s}^{-2}] \tag{4}$$

where: $E_{BL} = \dfrac{m_{BL} \cdot V_{BL}^2}{2}, \quad \dfrac{A \cdot m_r \cdot V_r^2}{2} = \dfrac{\sum\limits_{i=1}^{n} m_{ri} \cdot V_{ri}^2}{2},$

$B \cdot m_r \cdot V_r = \sum\limits_{i=1}^{n} m_{ri} \cdot V_{ri} \cdot \cos\phi_i,$

$m_r = \sum\limits_{i=1}^{n} m_{ri}, \quad M_{ew} = J/l^2, \quad V_r = \max V_{ri} \cdot \cos\phi_i, \quad V_w = l \cdot \omega_w,$

$m_r = m_{rp} + m_{rt}, m_s = m_{sp} + m_{st}.$

Preliminary analysis of the impact effects may be carried out at the following conditions:

$A = B$, where: $\cos\phi_i = \dfrac{V_{ri}}{V_r}$, and $A = B = 1$, where: $\cos\phi_i \cong 1$ and $V_{ri} \cdot \cos\phi_i \cong V_r$ at $\varphi < 10°$.

Then, the above equations take the form

$$m_p \cdot V_p - m_s \cdot V_w - m_r \cdot V_r = I, \text{[kgms}^{-1}] \tag{2a}$$

$$\frac{m_p \cdot V_P^2}{2} = \frac{m_{BL} \cdot V_{BL[Z]}^2}{2} + \frac{m_r \cdot V_r^2}{2} + \frac{I^2}{2M_{ew}}, \text{[kgm}^2 \text{s}^{-2}] \tag{4a}$$

Ballistic energy $E_{BL[Z]}$ is expressed by

$$E_{BL[Z]} = \frac{m_p \cdot V_p^2}{2} - \frac{1}{2m_r} \cdot (m_p \cdot V_p - I - m_s \cdot V_w)^2 - \frac{I^2}{2M_{ew}}, \text{[kgm}^2 \text{s}^{-2}] \tag{5}$$

without measurement of residual velocity V_r, and ballistic energy $E_{BL[Z1]}$ is expressed by

$$E_{BL[Z1]} = \frac{m_p \cdot V_p^2}{2} - \frac{V_r}{2}(m_p \cdot V_p - I - \frac{I \cdot m_s}{M_{ew}}) - \frac{I^2}{2M_{ew}}, \text{[kgm}^2 \text{s}^{-2}] \tag{6}$$

without measurement of residual mass m_r and at $A = B$.

Equivalent ballistic mass m_{BL} is determined from the relation

$$m_{BL} = m_p - \frac{I^2}{M_{ew} \cdot V_{BL}^2}, [\text{kg}] \qquad (7)$$

where: $V_{BL} = V_p$ and $V_r = 0$.

Ballistic velocity $V_{BL[Z]}$ of elastoplastic materials, where the mass $m_r \cong m_p \cong m_{BL}$ and without measurement of residual velocity V_r, takes the form

$$V_{BL[Z]} = [\frac{I}{m_p^2}(2m_p \cdot V_p - I)]^{1/2}, [\text{ms}^{-1}] \qquad (5a)$$

Ballistic velocity $V_{BL[Z1]}^2$, where $m_p \cong m_{BL}$, $m_s << M_{ew}$ and without measurement of residual mass m_r, takes the form

$$V_{BL[Z1]} = [V_p^2 - \frac{V_r}{m_p}(m_p \cdot V_p - I)]^{1/2}, [\text{ms}^{-1}] \qquad (6a)$$

The ballistic velocities are determined according to the author's method and ballistic velocity

$$V_{BL[R]} = [V_p^2 - V_r^2]^{1/2}, [\text{ms}^{-1}] \qquad (8)$$

is determined according to Recht's and Ipson's method [8, 9].

3. Experimental verification of ballistic resistance of the shields

The unified test stand for investigation of materials ballistic resistance was developed in the Polish Naval Academy in Gdynia and then co-patented by the author [1], with possibility of the work in field conditions (Fig. 1). Construction of the stand is based on the ballistic pendulum fitted to measure the impact forces of the shield, impact velocity V_p and residual velocity V_r of the projectile. The sample-target of 50 mm or 120 mm diameter is fastened on the front surface of the dynamometer. Impact of the projectile against the sample-target causes their deformation, simultaneously transferring a part of energy and momentum to the dynamometer, where the impact force $F(t)$ is registered. Optoelectronic and electrical dual-gate arrangement of 200 mm base is used to measure the projectile velocity with an average measurement uncertainty of 1%. It causes that the pendulum turns around the axis, where the turn angle of the pendulum χ is registered. All converted input quantities are transmitted to a digital oscilloscope and a personal computer.
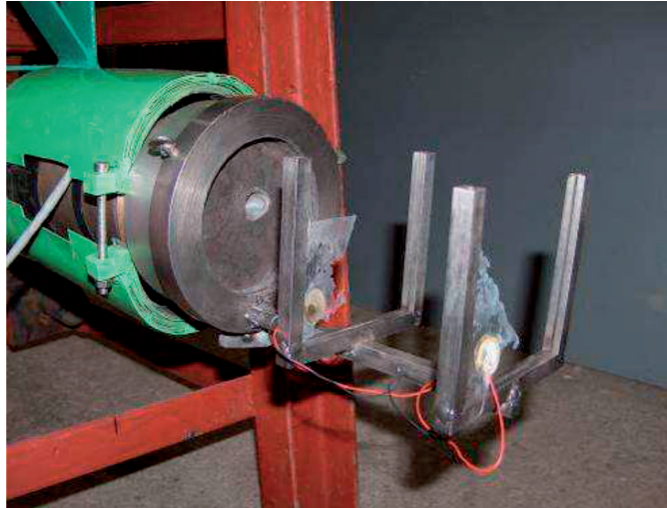
Fig. 1. The unified test stand for investigation of the materials ballistic resistance

The solution to equations (1-4) with respect to the impulse of force I transmitted to the dynamometer takes the form of a sinusoidal function of the turn angle χ

$$2 \sin \frac{\chi}{2} = \frac{I \cdot l^{3/2}}{J \cdot g^{1/2}} = \frac{\omega_w \cdot l^{1/2}}{g^{1/2}} \tag{9}$$

and is proportional to the angular velocity ω_w of the ballistic pendulum.

The author assumes the following method for calculating of the loading force impulse:

$$I = \int_0^{T_m} F(t) \cdot dt, [\text{Ns}] \tag{10}$$

and the impulse of unloading force

$$I_{od} = \int_{T_m}^{T^*} F(t) \cdot dt, [\text{Ns}] \tag{11}$$

where: $F(t)$ – the impact force is registered from oscilloscope, [N],

T$_m$ – time at maximum impact force, F$_{max}$, [s],

T* – time at zero unloading force, F = 0, [s].

For sinusoidal approximation of the impact force

$$F(t) = F_{\max.} \cdot \sin(\frac{\pi \cdot t}{2 \cdot T_m}), [\text{N}] \tag{12}$$

and the impulse of force transmitted to the dynamometer is expressed as

$$I = \frac{2 \cdot F_{\max.} \cdot T_m}{\pi}, [\text{Ns}] \tag{13}$$

The energy absorbed by the shield is calculated at the impact and residual velocity of the projectile and the impulse of impact force transmitted to the dynamometer.

The results of experiments, performed for determination of the shields ballistic resistance, indicate that the proper energy absorbed by the shield $V^2_{BL[R]}$, determined according to Recht's and Ipson's method, is less accurate than $V^2_{BL[Z]}$ calculated according to the author's method [5-7]. The introduced diagnostics method can be used for verification of numerical simulation of the projectile impact on homogeneous plates and multi-layered constructional shields [4, 10, 11].

4. Verification of numerical simulation

If properly validated, the finite element-based contact-impact analysis can be considered as the most potent approach for predicting ballistic limits of armour plates and for optimized design as well as innovative solutions.

In the Johnson-Cook material constitutive model [2], the effect of strain rate on yield stress and failure strain was considered; however, thermal effects were not accounted for

$$\bar{\sigma} = [A + B(\bar{\varepsilon})^n] \cdot \left[1 + C \ln\left(\frac{\dot{\bar{\varepsilon}}}{\dot{\bar{\varepsilon}}_0}\right)\right] \cdot \left[1 - \left(\frac{T - T_0}{T_m - T_0}\right)^m\right] \qquad (14)$$

at $T = T_0$, where:

$\bar{\sigma}$ – effective flow stress [MPa],

$\bar{\varepsilon}$ – effective plastic strain,

$\dot{\bar{\varepsilon}}_0$ – reference strain rate [$1s^{-1}$],

$\dot{\bar{\varepsilon}}$ – effective plastic strain rate [s^{-1}],

T – temperature of the material [°C],

T_m – melting point of the material [°C],

T_0 – reference temperature [°C],

A, B, C, m, n – experimental constants.

For the impact velocities considered here, which are well in the ordnance range, the computed results are not expected to be substantially influenced by this latter assumption.

Mechanical properties of the quenched and tempered 10GHMBA-E620T steel were developed from static tensile test carried out on the material testing system MTS810-12. Dynamic tension tests were carried out with the use of rotational hammer of maximum strain rate $\dot{\bar{\varepsilon}} = 10^3 s^{-1}$.

The paper describes simulation of a steel plate impacted by a projectile using explicit finite element analysis implemented in the Ansys (LS Dyna).

The effective flow stress distribution for the steel sample-target of 32 mm thickness impacted by the 12,7 mm type Rigid Body(RB) projectile is shown in Fig. 2.
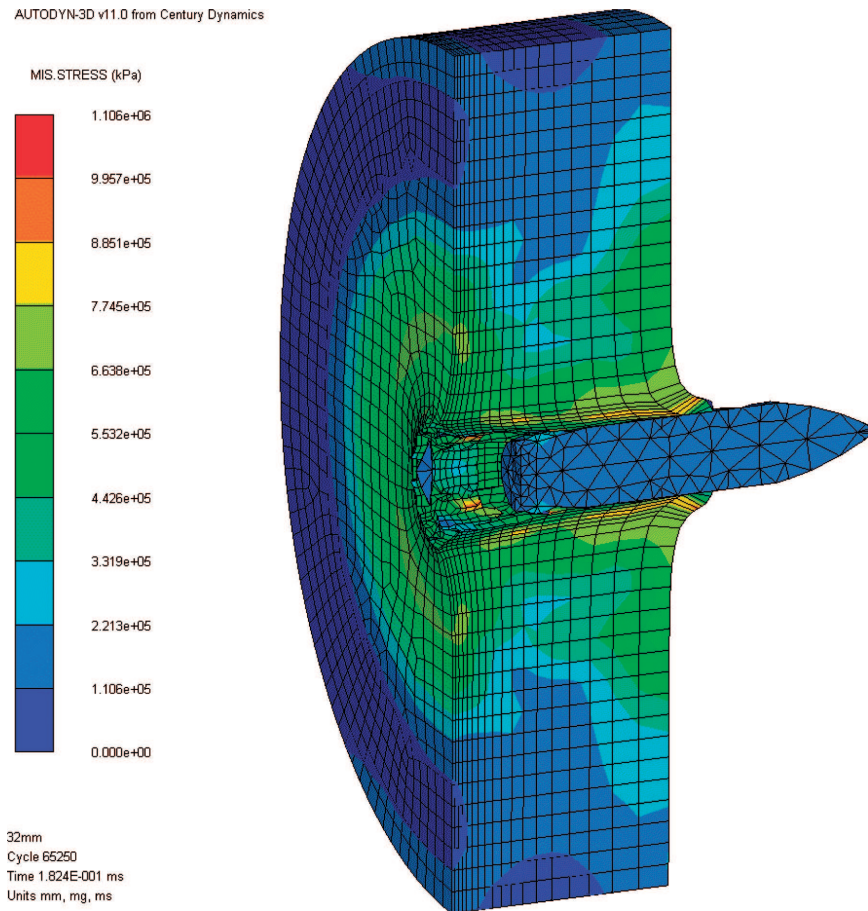

Fig. 2. The effective flow stress distribution for the steel sample-target of 32 mm thickness impacted by the 12,7 mm type RB projectile (LS Dyna) [3]

All analyses were carried out with the explicit contact-impact LS Dyna analysis code. Validation of the numerical modelling includes comprehensive hexagonal mesh convergence study, with the use of axisymmetric elements representing target plates. The ballistic velocity $V_{BL} = VBO$ of the 10GHMBA-E620T steel plates impacted by the deformable 12,7 mm type B-32 projectile was computed with the use of validated numerical procedure and experimental tests [3]. The ballistic velocities: $V_{BL[Z1]}, V_{BL[Z]}, V_{BL[RI]}$ were obtained from experiments according to the equations 5a, 6a and 8. Verification of the numerically simulated ballistic velocity VRO is shown in Figure 3.
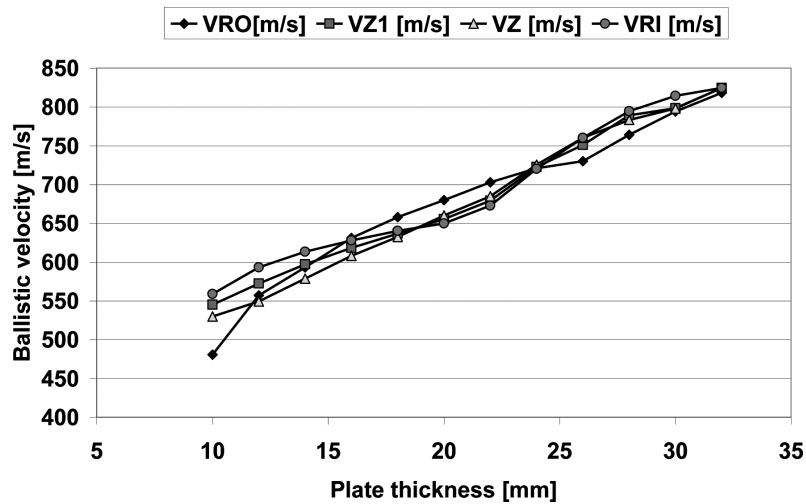
Fig. 3. Comparison of experimentally-determined ballistic velocities: $V_{BL[Z1]}, V_{BL[Z]}, V_{BL[RI]}$ with numerically-simulated ballistic velocity *VRO* of the 10GHMBA-E620T steel shield impacted by the 12.7 mm type B-32 projectiles

The experimentally-determined ballistic velocities $V_{BL[Z1]}$ (*VZ*) and $V_{BL[Z1]}$ (*VZ1*), according to the author's method, and ballistic velocity $V_{BL[RI]}$(*VRI*), according to Recht's and Ipson's method, are compared with the numerically-simulated ballistic velocity *VRO* in Figures 4-6. The 10GHMBA-E620T steel shield of 32 mm ballistic thickness impacted by the 12.7 mm type B-32 pro-jectile is tested at the ballistic velocity of $V_B = 824{,}0$ ms^{-1} and the kinetic energy of 17 kJ.
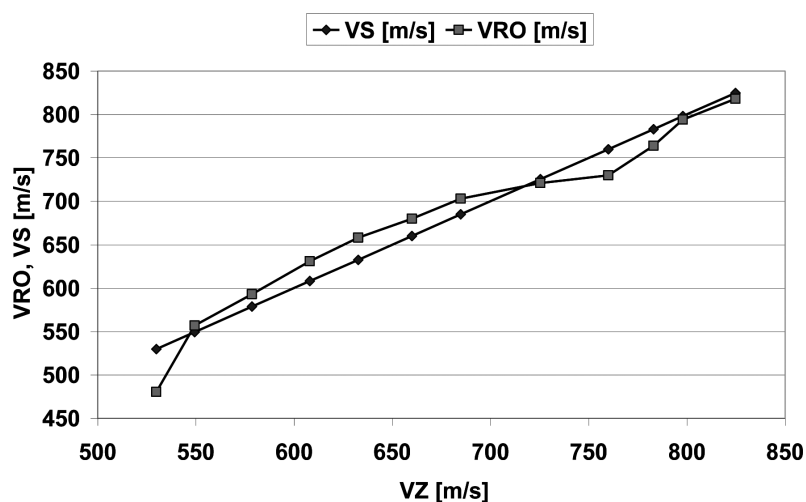

Fig. 4. Comparison of the experimentally-determined ballistic velocity $V_{BL[Z]}$(*VZ=VS*) with the numerically-simulated ballistic velocity *VRO* of the 10GHMBA-E620T steel shield impacted by the 12.7 mm type B-32 projectiles (correlation coefficient *R = 0,9734*)

The modelling requirements are derived by correlating the published test ballistic velocities for variants of steel plates of different thicknesses at impact velocities in the range of ~820-870 m/s. Effectiveness of the author's method is better than the Recht's and Ipson's method for determination of the ballistic velocity. The methodology used in this paper for obtaining ballistic velocity may be useful in other applications, e. g. low velocity impact on a steel plate distinct from ballistic impact of the reference material.
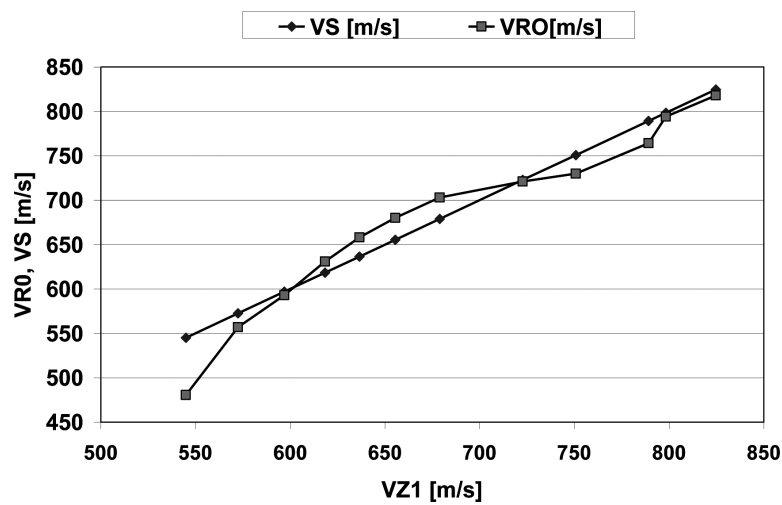

Fig. 5. Comparison of the experimentally-determined ballistic velocity $V_{BL[Z1]}$ ($VZ1 = VS$) with the numerically-simulated ballistic velocity VRO of the 10GHMBA-E620T steel shield impacted by the 12.7 mm type B-32 projectiles (correlation coefficient $R = 0,9677$)
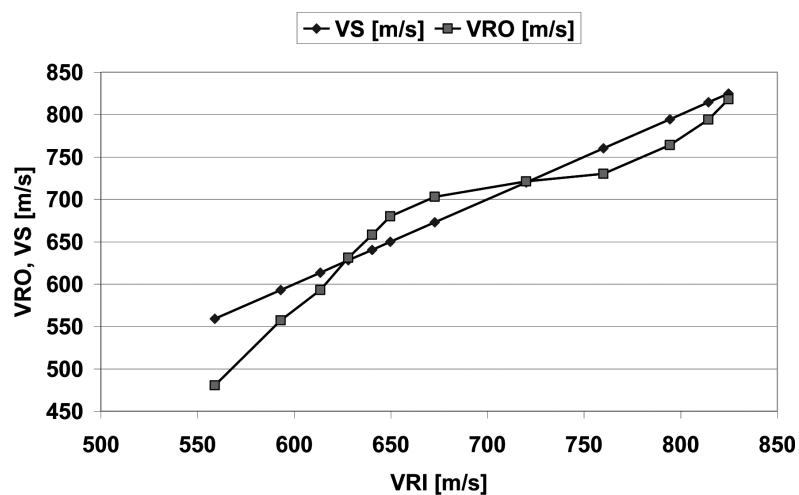

Fig. 6. Comparison of the experimentally-determined ballistic velocity $V_{BL[RI]}$ ($VRI = VS$) with the numerically-simulated ballistic velocity VRO of the 10GHMBA-E620T steel shield impacted by the 12.7 mm type B-32 projectiles (correlation coefficient $R = 0,9510$)

The modelling guidelines developed in this paper can thus be useful in efficient creating of new design solutions, which can otherwise need considerably more time and resources if determined by physical testing.

5. Summary

The energy absorbed by the shield is calculated from measurement of the impact and residual velocity of the projectile and the impulse of force transmitted to the dynamometer.

The results of high-strength steel ballistic resistance obtained in the numerical simulation were compared with experimental tests at the unified test stand. For the ballistic velocity, the effectiveness of the author's method is better than that of the Recht's and Ipson's method.

Experimental verification of the numerical simulation of projectile impact on ballistic shields is a basic advantage of the method and the presented unified test stand. For a number of cases, if one takes a proper choice of contact algorithm, element size, as well as temperature as and strain rate-dependent material properties, the computed projectile ballistic velocities can match closely the corresponding test-based values.

When the confidence in the modelling procedures which could yield converged ballistic velocity for single-layered plates is established, one may carry out a number of studies by varying plate thickness, projectile parameters and, impact velocity of multi-layered shields.

Acknowledgment

REFERENCES

[1] Fila J., Zatorski Z.: The unified test stand for investigation of materials ballistic resistance, especially for ship, constructional and armour shields, Patent Nr 0641, 1998, AMW Gdynia. (in Polish)

[2] Johnson G.R., Cook W.H.: A constitutive model and data for metals subjected to large strains, high strain rates and high temperatures, Proceedings of the 7th International Symposium of Ballistics, The Hague, The Netherlands, 1983, pp. 541-547.

[3] Szturomski B. i in.: Dynamic characteristics of ship materials for verification of numerical simulation of anti-terroristic shields, AMW Gdynia, 2009, (unpublished). (in Polish)

[4] Zatorski Z.: Design of ballistic multi-layered steel shields, Marine Technology Transactions, 2006, Vol. 17, pp. 189-199.

[5] Zatorski Z.: Diagnostics of ballistic resistance of constructional shields and experimental verification, Journal de Physique IV France, 2006, Vol. 134, pp. 1131-1135.

[6] Zatorski Z.: Diagnostics of ballistic resistance of multi-layered shields and fracture mechanisms, Multi-phase and multi-component materials under dynamic loading, 10th European Mechanics of Materials Conference (EMMC10), Kazimierz Dolny, Poland, June 11-14, 2007, Eds. W. K. Nowacki and Han Zhao, IFTR PAS, Warsaw and LMT Cachan, pp. 441-450.

[7] Zatorski Z.: Diagnostics of ballistic resistance multi-layered shields, The Archive of Mechanical Engineering, 2007, Vol. LIV, No. 3, pp. 205-218.

[8] Zatorski Z.: Modelling and experimental verifications of energy absorbed by constructional shields under firing, The Archive of Mechanical Engineering, 2007, Vol. LIV, No. 1, pp. 17-25.

[9] Zatorski Z.: Modelling of energy absorbed of homogenous plates under firing, Marine Technology Transactions, 2005, Vol. 16, pp. 317-328.

[10] Zatorski Z.: Ballistic resistance of ceramic-rubber-steel composite, Zeszyty Naukowe Akademii Marynarki Wojennej, 2005, Nr 1, pp. 219-227. (in Polish)

[11] Zatorski Z.: Ballistic resistance of ceramic-laminate composite, Zeszyty Naukowe Akademii Marynarki Wojennej, 2005, Nr 2, pp. 139-149. (in Polish)

Eksperymentalna weryfikacja symulacji numerycznej ostrzału osłon balistycznych

Streszczenie

W prezentowanej pracy opracowano weryfikację eksperymentalną symulacji numerycznej ostrzału osłon konstrukcyjnych. Eksperymentalne testy przeprowadzono na zunifikowanym stanowisku do badania w warunkach polowych odporności balistycznej materiałów. Stanowisko badawcze opracowano w Akademii Marynarki Wojennej w Gdyni, a następnie opatentowano. Projekt stanowiska oparto na konstrukcji wahadła balistycznego oprzyrządowanego w układy do pomiaru siły uderzenia, prędkości początkowej i resztkowej pocisku oraz kąta obrotu wahadła χ. Wszystkie dane pomiarowe były przenoszone do oscyloskopu cyfrowego i komputera PC. Prędkości balistyczne osłony $V_{BL[R]}$ wyznaczone zgodnie z metodą Rechta-Ipsona porównano z prędkościami $V_{BL[Z]}$ i $V_{BL[Z1]}$ wyznaczonymi zgodnie z metodą autora. Weryfikację symulowanej numerycznie prędkości balistycznej wobec powyższych prędkości oparto na wynikach ostrzału osłon ze stali 10GHMBA-E620T pociskami B-32 kal. 12,7 mm. Wprowadzona metoda może być użyta równocześnie do określenia prędkości balistycznej V_{BL} i grubości balistycznej h_{BL} osłon jednorodnych i wielowarstwowych.